TẠP CHÍ KHOA HỌC
TRƯỜNG ĐẠI HỌC SƯ PHẠM TP HỒ CHÍ MINH
Tập 23, Số 3 (2026): 644-656
Website: https://journal.hcmue.edu.vn
ISSN: 2734-9918

HO CHI MINH CITY UNIVERSITY OF EDUCATION
JOURNAL OF SCIENCE
Vol. 23, No. 3 (2026): 644-656
https://doi.org/10.54607/hcmue.js.23.3.4408(2026)

Research Article

ENHANCING THE ADSORPTION CAPACITY OF Pb^{2+} AND Cu^{2+} IONS IN AQUEOUS SOLUTION USING POTASSIUM PERMANGANATE-MODIFIED BIOCHAR

Luu Gia Hy[1], Pham Tang Cat Luong[2], Truong Chi Hien[1], Nguyen Thi Bach Mai[3], Nguyen Kim Diem Mai[1*]

[1]Ho Chi Minh City University of Education, Vietnam
[2]Ho Chi Minh City University of Technology, Vietnam National University, Ho Chi Minh City, Vietnam
[3]Nong Lam University of Ho Chi Minh City, Vietnam
[*]Corresponding author: Nguyen Kim Diem Mai – Email: mainkd@hcmue.edu.vn
Received: July 09, 2024; Revised: September 08, 2024; Accepted: October 01, 2024

ABSTRACT

This study aims to enhance the adsorption capacity of sawdust-derived biochar (BC-MC) for heavy metal ions by modifying it with a $KMnO_4$ solution. The adsorption performance of $KMnO_4$-modified biochar (BC-$KMnO_4$) was evaluated by examining the impact of various single-variable factors: pH (2.0 – 6.0), initial concentration of the metal ions (25 – 200 mg·L^{-1}), adsorption time (5 – 1440 minutes), and adsorbent mass (0.05 – 0.10 g). The findings indicate that the adsorption of Cu^{2+} and Pb^{2+} ions onto BC-$KMnO_4$ followed the pseudo-second-order kinetic model and the monolayer adsorption mechanism, suggesting that the Langmuir adsorption isotherm model best describes the adsorption process. The BC-$KMnO_4$ exhibited a maximum adsorption capacity of 24.15 mg·g^{-1} for Cu^{2+} and 90.09 mg·g^{-1} for Pb^{2+}. Overall, the study confirms that $KMnO_4$ modification significantly enhances the adsorption capacity of BC-MC for metal ions, making it a promising low-cost and environmentally friendly material for water treatment applications.

Keywords: adsorption; biochar; ion Cu^{2+}; ion Pb^{2+}; modification with $KMnO_4$

1. Introduction

With the rapid development of industrial activities, a large amount of industrial wastewater containing heavy metals is discharged into water resources, leading to significant environmental problems (Barakat, 2011). Heavy metals such as Pb, Cu, and Cd are often highly toxic, non-biodegradable, and accumulate in soil, water, and living organisms, posing a severe threat to human health (Kumar et al., 2014). Therefore, developing effective methods for treating metal-contaminated wastewater before it is discharged into the natural environment is an urgent priority.

Cite this article as: Luu, G. H., Pham, T. C. L., Truong, C. H., Nguyen, T. B. M., & Nguyen, K. D. M. (2026). Enhancing the adsorption capacity of Pb^{2+} and Cu^{2+} ions in aqueous solution using potassium permanganate-modified biochar. *Ho Chi Minh City University of Education Journal of Science, 23*(3), 644-656. https://doi.org/10.54607/hcmue.js.23.3.4408(2026)

Various methods have been employed for the removal of heavy metal ions from water, including chemical precipitation, electrochemical treatment, ion exchange, and photochemical methods. However, most of these methods are expensive and involve complex procedures. Among these methods, adsorption is considered a relatively low-cost and highly efficient method for treating wastewater with low heavy metal content (Sun et al., 2019). Amongst adsorbent materials, biochar has received significant research attention due to its favorable surface properties for adsorption, such as its porous structure and the presence of active functional groups that can complex, chelate, and interact with metal ions (Duwiejuah et al., 2017). However, the treatment capacity of raw biochar is often low due to its smaller surface area compared to activated carbon and limited functional groups (Tan et al., 2016). Therefore, research on modifying biochar to enhance its treatment capacity is essential. Previous studies have shown that manganese oxides (MnO_x) have a good ability to bind heavy metal ions. The addition of MnO_x can significantly increase the number of complexing functional groups on the surface of the material (Song et al., 2014), thereby enhancing the interaction between heavy metal ions and biochar through the formation of complexes with these functional groups (Wang et al., 2015).

Based on this, the study focuses on enhancing the heavy metal adsorption capacity of sawdust-derived biochar using a modification method with potassium permanganate solution. This method is simple and easy to implement, aiming to increase the active functional groups on the biochar's surface and supplement it with manganese oxide particles that have the ability to bind with heavy metals.

2. Materials and methods

2.1. Material preparation

Sawdust samples were collected from Tien Thuy commune, Chau Thanh district, Ben Tre province. The collected sawdust was dried at 110°C for 24 hours to remove all moisture and then ground into fine particles before use. This process was carried out similarly to the previous study by Pham et al. (2021).

2.2. Chemicals, Equipment, and Devices

The chemicals used were of high purity from Merck and China (purity > 99,9%), including $Pb(NO_3)_2$, $Cu(NO_3)_2 \cdot 3H_2O$, $KMnO_4$, KCl, HNO_3, NaOH, HCl, NH_3 25%, pH 4.01, and 7.00 buffer solutions. Standard solutions of Pb^{2+} 1000 $mg \cdot L^{-1}$ and Cu^{2+} 1000 $mg \cdot L^{-1}$ was also used. Deionized (DI) water was prepared in the laboratory by using a WATER PRO PS device.

The equipment used included a Thermo Scientific (USA) iCE 3000 SERIES AAS,, Dragonlab (USA) SKO300-Pro rotary shaker, a Nabertherm oven, a Memmert-UNB500 drying oven, and an SI Analytics pH meter.

2.3. Experimental Design

2.3.1. Production of biochar

Biochar was produced following a procedure similar to that described in a previous study (Pham et al., 2021). Specifically, the treated sawdust was pyrolyzed under a nitrogen

atmosphere at 400 °C for 2 hours. After cooling to room temperature, the product was washed repeatedly with acetone to remove organic matter and then with deionized (DI) water until the pH of the wash water was approximately 7.0. The biochar was then dried overnight at 80 °C and stored in a desiccator. This biochar sample was denoted as BC-MC.

2.3.2. Biochar modification

A total of 2.0 g of BC-MC was added to 100 mL of 0.01 M $KMnO_4$ solution and stirred continuously for 6 hours. The solid product was then filtered, washed with deionized (DI) water, and dried completely at 60 °C. The modified biochar was denoted as BC-$KMnO_4$. Figure 1 illustrates the biochar modification process.

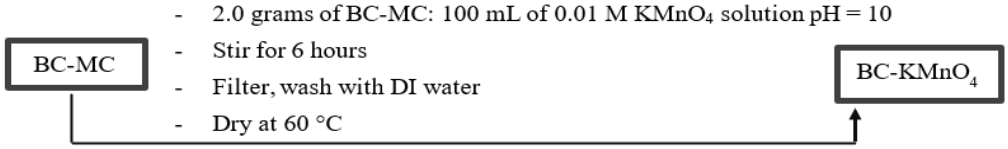

Figure 1. *Schematic diagram of the modification process using $KMnO_4$ solution*

2.3.3. pH_{pzc} survey experiment

The point of zero charge (pzc) for a material surface is the pH value of the solution at which the material surface charge is zero. In the study of material surfaces, pzc is used as a tool to explain ion exchange and adsorption processes on the material surface (Bakatula et al., 2018). In this study, the pH drift method was used to measure the pH_{pzc} on the biochar surface because it was found to be the most commonly used and reliable method in recent studies. This method is based on the difference between the pH values of the solution before and after ion exchange with the material being studied. The pH_{pzc} value is the pH at which $\Delta pH_i = 0$.

$$\Delta pH_i = pH_{final} - pH_{initial} \quad (1)$$

where pH_{final}: pH value of the solution after ion exchange with the investigated material.

$pH_{initial}$: pH value of the solution before ion exchange with the investigated material.

To determine the pH_{pzc} of BC-$KMnO_4$, triangular flasks containing 40 mL of 0.1 M $NaNO_3$ solution were prepared with initial pH values from 3.0 to 11.0 ($pH_{initial}$ adjusted with 0.1 M HNO_3 and 0.1 M NaOH). Then, 0.05 grams of BC-$KMnO_4$ was added to each triangular flask, and the suspensions were shakencontinuously for 24 hours at 200 round per minute. After filtration, the final pH values were measured. The data were processed to determine the pH_{pzc} value.

2.3.4. Design of single-variable experiments to investigate the factors of initial solution pH, adsorption time, concentration of metal ions, and BC-$KMnO_4$ mass

To facilitate the comparison of results, the conditions for investigating the factors affecting the adsorption capacity of Pb^{2+}, Cu^{2+} ions by BC-$KMnO_4$, including initial solution pH, adsorption time, initial concentration of metal ions, and mass of adsorbent, were adopted from a previous study (Pham et al., 2021). The volume of the solution is kept constant at 50 mL, while the remaining experimental conditions are shown in Table 1.

Table 1. *Experimental conditions for investigating factors affecting BC-$KMnO_4$*

Factor	BC-$KMnO_4$ mass (g)	pH	Initial concentration ($mg \cdot L^{-1}$)	Adsorption time (minutes)	Shaking speed (rpm)
pH	*0.05*	*2.0 – 6.0*	*50 (Pb), 25 (Cu)*	*120*	*500*
Time	*0.05*	*4.0*	*50 (Pb), 25 (Cu)*	*5 – 1440*	*500*
Concentration	*0.05*	*4.0*	*5 - 200*	*120*	*500*
BC-$KMnO_4$ mass	*0.02 – 0.10*	*4.0*	*100 (Pb), 50 (Cu)*	*120*	*500*

The experiments were repeated three times, and the average value was taken. The adsorption capacity of metal ions on BC-$KMnO_4$ was calculated according to equation (2):

$$Q = \frac{(C_o - C_t) \cdot V}{m} \quad (2)$$

where Q is the adsorption capacity ($mg \cdot g^{-1}$); C_o is the initial concentration of metal ions ($mg \cdot L^{-1}$); C_t is the final concentration of metal ions ($mg \cdot L^{-1}$); V is the volume of the solution (L) and m is the mass of BC-$KMnO_4$ (g).

2.3.5. Investigation of competitive adsorption of Cu^{2+} and Pb^{2+} ions onto BC-$KMnO_4$

To evaluate the competitive adsorption of the BC-$KMnO_4$ material for Cu^{2+} and Pb^{2+} ions, 0.05 g of BC-$KMnO_4$ was weighed and added to 50 mL of a solution containing a mixture of Cu^{2+} and Pb^{2+} ions at the same concentration of 100 $mg \cdot L^{-1}$, the pH of the solution was adjusted to 4.0, and shaken continuously for 2 hours using a magnetic stirrer.

The concentrations of ions before and after adsorption were determined, and the adsorption capacity was evaluated using equation (2). The experiments were repeated three times, and the average values were taken.

2.3.6. Investigation of adsorption kinetics and isotherm models for the adsorption process

Based on the experimental adsorption data, data analysis were performed to find the kinetic equation that describes the adsorption rate and the appropriate adsorption isotherm model for the adsorption of Cu^{2+} and Pb^{2+} ions on BC-$KMnO_4$.

These equations are described in detail in Table 2 (Atkins, 2013; Inyang et al., 2012b; Ni et al., 2019; Xiao et al., 2019).

Table 2. *Description of linear equations for adsorption kinetic models and adsorption isotherm models*

Model		Corresponding equation	Parameters and units
Adsorption kinetics	***First-order***	$ln(Q_e - Q_t) = ln(Q_e) - k_1 \cdot t$	Q_e: equilibrium adsorption capacity ($mg \cdot g^{-1}$) Q_t: adsorption capacity at time t ($mg \cdot g^{-1}$) Q_{max}: maximum adsorption capacity ($mg \cdot g^{-1}$) C_e: equilibrium concentration of adsorbate ($mg \cdot L^{-1}$) k_1: first-order kinetic constant (min^{-1}) k_2: second-order kinetic constant ($g \cdot mg^{-1} \cdot min^{-1}$) K_L: Langmuir constant ($L \cdot mg^{-1}$). K_F: Freundlich constant ($mg \cdot g^{-1}$) n: adsorption intensity
	Second-order	$\frac{t}{Q_t} = \frac{1}{k_2 . Q_e^2} + \frac{t}{Q_e}$	
Adsorption isotherm	***Langmuir***	$\frac{C_e}{Q_e} = \frac{1}{Q_{max}} . C_e + \frac{1}{Q_{max} . K_L}$	
	Freundlich	$lnQ_e = lnK_F + \frac{1}{n} lnC_e$	

2.3.7. Material morphology and properties study

The surface characteristics and morphology of the material were determined based on scanning electron microscopy (SEM) images on a FE-SEM S4800 HITACHI-Japan machine at the Nanotechnology Lab - High-Tech Park Research and Development Center, Ho Chi Minh City.

The specific surface area was measured by the Brunauer-Emmett-Teller (BET) method using a Nova 1000e device at the Applied Materials Science Institute.The weight percentages of the elements in the coal samples before and after adsorption were determined by X-ray energy-dispersive spectroscopy (EDX), using an EDX H-7593 HORIBA-UK machine at the same location. EDX spectra were determined at three different positions, and the average value was reported.

The infrared spectra were measured using a Jasco FT-IR infrared spectrometer in the Central Laboratory, Faculty of Chemistry, Ho Chi Minh City University of Education.

3. Results and discussion

3.1. Characteristics of biochar

The specific surface area (BET method) of BC-MC and BC-$KMnO_4$ reached 115.40 and 61.33 $m^2 \cdot g^{-1}$, respectively. Thus, it can be seen that there was a significant decrease in the value of BC-$KMnO_4$ compared to BC-MC. On the other hand, when comparing the surface morphology of the BC-$KMnO_4$ and BC-MC materials, respectively shown in Figures 2a and 2b, it can be seen that the multi-layered, grooved structure of the surface of the initial BC-MC material was broken down and became blocks with a relatively smoother surface on the surface of BC-$KMnO_4$. This helps to explain why the surface area value of BC-$KMnO_4$ decreased significantly compared to BC-MC.

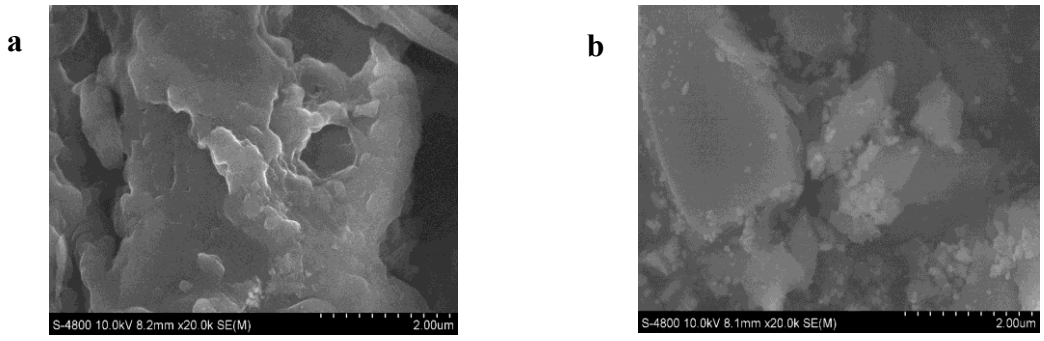

Figure 2. *SEM images of BC-MC (a) and BC-$KMnO_4$ (b)*

In addition, in Figure 2b, small particles can be seen adhering to the surface of the material. These particles may be manganese oxide particles generated from the material modification process. This result is similar to that of Zhengguo Song's research (Song et al., 2014).

The FT-IR spectra are shown in Figure 3. A comparison of the FT-IR spectra of BC-MC and BC-$KMnO_4$, together with the results reported in a previous study (Pham et al., 2021) and Figure 3a, shows that the signal in the wavenumber range of 2700–3200 cm^{-1} for BC-$KMnO_4$ differs from that of BC-MC. This is the signal region attributed to the vibration of the -OH group, indicating that the -OH group of BC-$KMnO_4$ has changed compared to BC-MC. This can be explained by the oxidation of the >C=C< bonds on the surface of BC-MC to >C-OH groups, as evidenced by the narrowing of the signal region from 1400 to 1500 cm^{-1}, a region attributed to the vibration of >C=C< groups. In addition, the signal at 1580 cm^{-1} attributed to the vibration of the C=O group also changes after modification, suggesting that >C=C< is not only oxidized to >C-OH but also partially to >C=O. On the other hand, the new signals at wavenumbers 637, 84, and 754,31 cm^{-1} that appear in the BC-$KMnO_4$ spectrum can be attributed to the vibration of bonds in MnO_x molecules (Keiluweit et al., 2010; Merck, 2022; Song et al., 2014; Xiao et al., 2019). This further confirms the presence of manganese oxide particles on the surface of the material in the SEM images.

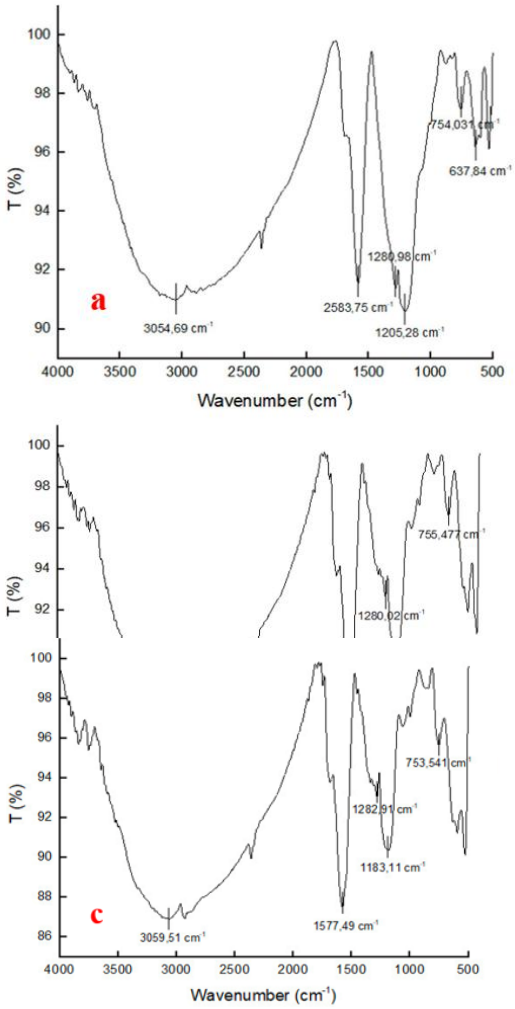

Figure 3. *FT-IR spectra of BC-$KMnO_4$ (a), BC-$KMnO_4$ after Cu^{2+} adsorption (b) and BC-$KMnO_4$ after Pb^{2+} adsorption* (c)

According to the data obtained from the EDX spectra in Table 3, a manganese signal is observed in BC-$KMnO_4$, which is absent in BC-MC.

Table 3. *EDX spectrum data of materials*

	Element mass percent (%)					
	C	***O***	***Ca***	***Mn***	***Cu***	***Pb***
BC-MC *(Pham et al., 2021)*	*75.55*	*23.09*	*1.36*	---	---	---
BC-$KMnO_4$	*68.36*	*27.20*	*0.81*	*3.64*	---	---
BC-$KMnO_4$ after Cu^{2+}adsorption	*67.78*	*29.24*	---	*1.86*	*1.12*	---
BC-$KMnO_4$ after Pb^{2+} adsorption	*70.05*	*23.03*	*0.86*	*2.58*	---	*3.48*

This partially proves that the modification process has taken place. After adsorption of Cu^{2+} and Pb^{2+} ions, the material composition showed the presence of signals of these two ions. This proves that the adsorption process of BC-$KMnO_4$ for these two ions has taken

place. Furthermore, the EDX spectrum of BC-$KMnO_4$ after Cu^{2+} ion adsorption reveals the absence of calcium element signals. Consequently, a potential mechanism for Cu^{2+} ion treatment can be inferred as an ion exchange adsorption process involving Ca^{2+} and Cu^{2+}, which has been proposed in prior research (Ma et al., 2021; Pham et al., 2021).

3.2. Results of the study of single-variable factors affecting the adsorption process

3.2.1. Effect of pH

pH is a significant factor; it greatly affects the adsorption capacity of the material as well as the competition of ions in the adsorption process. Therefore, studying the effect of pH on the adsorption process is necessary. The results of the investigation of this factor are shown in Figure 4.

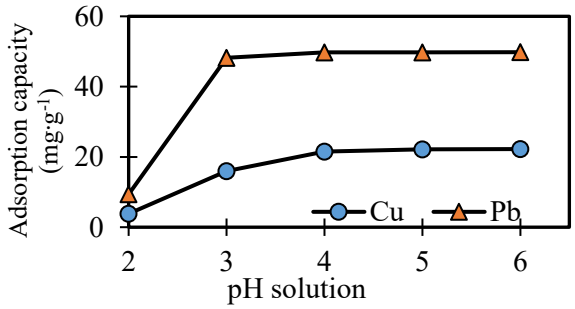

Figure 4. *Adsorption capacity of Cu^{2+} and Pb^{2+} ions onto BC-$KMnO_4$ as a function of pH*

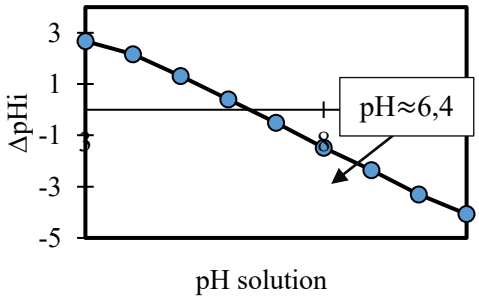

Figure 5. *ΔpH_i as a function of pH solution of BC-$KMnO_4$*

In general, as the solution pH increases, the adsorption capacity of BC-$KMnO_4$ for both metal ions also increases. This can be explained by the fact that the isoelectric point pH_{pzc} of this material is around 6.4 (as shown in Figure 5). At pH values below 6.4, the surface becomes increasingly positively charged, enhancing electrostatic repulsion between metal cations and the material surface, thereby reducing the adsorption capacity (Y. Wang et al., 2018). On the other hand, increasing the pH decreases the concentration of H^+ ions in the solution, thereby reducing competition between H^+ ions and metal cations for adsorption sites. In addition, this limits the protonation of functional groups involved in complexation with metal cations. This result is consistent with some previous studies (Song et al., 2014; Sun et al., 2019). When the solution pH increases from 2.0 to 3.0, the adsorption capacity increases rapidly from 3.83 to 16.01 $mg \cdot g^{-1}$ for Cu^{2+} ions and from 9.37 to 48.17 $mg \cdot g^{-1}$ for Pb^{2+} ions. When the pH continues to increase from 3.0 to 4.0, the adsorption capacity for Cu^{2+} ions continues to increase sharply, specifically from 16.01 to 21.52 $mg \cdot g^{-1}$, while for Pb^{2+} ions it only increases slightly from 48.17 to 49.73 $mg \cdot g^{-1}$. When the pH reaches 4.0 or higher, the adsorption capacity remains almost unchanged, and the pH range of 4.0 – 6.0 can be considered optimal for the adsorption process.

3.2.2. Effect of time

An experimental study was conducted to investigate the adsorption of Cu^{2+} and Pb^{2+} ions by BC-$KMnO_4$ at different time intervals of 5, 15, 30, 45, 60, 90, 120, 180, 240, and 1,440 minutes. The experimental results are shown in Figure 6.

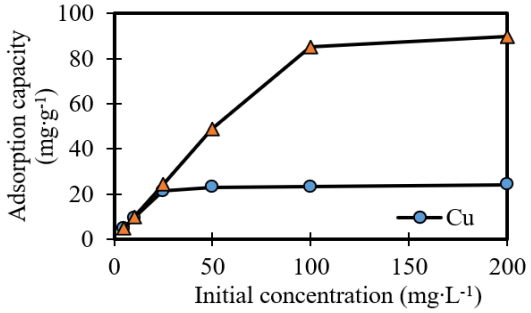

Figure 7. *Adsorption capacity of Cu^{2+} and Pb^{2+} ions onto BC-$KMnO_4$ as a function of initial concentration ions onto BC-$KMnO_4$ over time*

The results demonstrate a gradual increase in the adsorption capacity of BC-$KMnO_4$ over time. Specifically, from 5 to 120 minutes, the adsorption capacity for Cu^{2+} and Pb^{2+} ions rapidly increases from 15.0 to near 20.8 mg·g^{-1} and from 46.23 to 49.72 mg·g^{-1}, respectively. As time increases, from 120 to 1440 minutes, the increase in the adsorption capacity of the material decreases significantly. For Cu^{2+} ions, the increase is only from 20.8 to 22.7 mg·g^{-1}, while for Pb^{2+} ions, the increase is from 49.72 to 49.78 mg·g^{-1}. This can be explained by the fact that in the early stages, the metal ions interact on the surface of the material, and adsorption mainly occurs on the surface of the material. After a period of time, the adsorption sites on the surface of the material become saturated, and then the remaining metal ions in the solution begin to penetrate deeper and interact with the active sites inside the material. This is where the adsorption process is slower (H. Li et al., 2017). Thus, 120 minutes is the chosen time for the adsorption process (H. Li et al., 2017).

3.2.3. Effect of concentration

An experimental study was conducted to investigate the adsorption of Cu^{2+} and Pb^{2+} ions by BC-$KMnO_4$ at corresponding initial concentration values of metal ions: 5, 10, 25, 50, 100, and 200 mg·L^{-1}. The results are shown in Figure 7.

At a determined and constant mass of activated carbon, meaning that the number of active adsorption sites on the material surface is constant, changing the initial concentration of the adsorption solutions gives us results on the rapid increase in adsorption capacity when the initial concentration increases from 5 to 25 mg·g^{-1} (for Cu^{2+} ions) and from 5 to 100 mg·g^{-1} (for Pb^{2+} ions). As the initial concentration continues to increase, the adsorption capacity increases more slowly. This can be explained by the fact that at an initial concentration of 25 mg·L^{-1} (for Cu^{2+} ions) and 100 mg·L^{-1} (for Pb^{2+} ions), the BC-$KMnO_4$ material has almost saturated the active sites on the surface, and the adsorption process is approaching equilibrium. This argument is similar to a previous study (Pham et al., 2021).

3.2.4. Effect of material mass

The results of the survey on the effect of material mass on the adsorption of Cu^{2+} and Pb^{2+} ions by BC-$KMnO_4$ are shown in Figures 8 and 9, respectively. The mass values investigated were 0.02, 0.03, 0.04, 0.05, 0.06, 0.08, and 0.10 g.

The results show that the trend of the graphs for both metal ions is relatively similar. Both graphs in the two figures show an increase in adsorption efficiency and a decrease in adsorption capacity with increasing material mass. This can be explained by the fact that the number of adsorption sites of the material is limited. At low material mass, there are few adsorption sites but a high content of adsorbate (metal ions), so the adsorption process takes place easily. Conversely, when examined at high material mass, there are more adsorption sites, the number of metal ions per unit surface area of the material decreases, or in other words, the material has been used in excess (Bui & Tran, 2017; Pham et al., 2021).

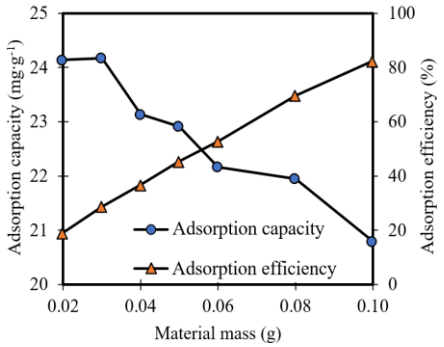

Figure 8. *Adsorption capacity and adsorption efficiency of Cu^{2+} ions onto BC-$KMnO_4$ as a function of material mass*

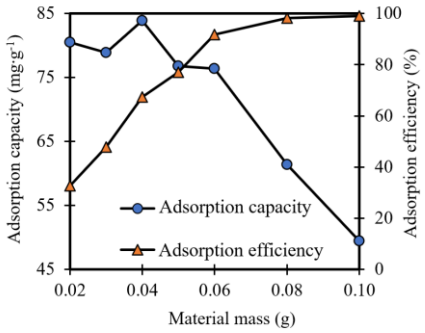

Figure 9. *Adsorption capacity and adsorption efficiency of Pb^{2+} ions onto BC-$KMnO_4$ as a function of material mass*

3.3. Investigation of adsorption kinetics and isotherm models

Based on the experimental data collected on the effect of time and initial concentration, the parameters of the adsorption kinetic and isotherm equations were analyzed and processed. The parameters of these equations were extrapolated and are presented in Table 4.

Upon examining each kinetic equation, it can be observed that the adsorption process of both Cu^{2+} and Pb^{2+} ions onto BC-$KMnO_4$ better fits the second-order kinetic model than the first-order kinetic model. This is reflected by the R^2 correlation coefficients of the derived second-order kinetic equations, which are 0.99 and 1.00 for Cu^{2+} and Pb^{2+} ions, respectively, compared to only 0.84 for Cu^{2+} ions and 0.76 for Pb^{2+} ions in the first-order kinetic equations. Alternatively, the discrepancy between the adsorption capacity value derived from the equations ($Q_{e,\,cal}$) and the experimental value ($Q_{e,exp}$) further supports this conclusion. These findings are consistent with previous studies (B. Li et al., 2017; Pham et al., 2021; Xiao et al., 2019).

Table 4. *Description of parameters for the kinetic and isothermal adsorption models of BC-$KMnO_4$ for Cu^{2+} and Pb^{2+} ion adsorption*

Model		Ion	Parameter 1	Parameter 2	Parameter 3	R^2
Kinetic adsorption	***First-order***	Cu^{2+}	$k_1 = 0.043$	$Q_{e,exp} = 22.73$	$Q_{e,cal} = 7.73$	0.84
		Pb^{2+}	$k_2 = 0.0115$	$Q_{e,exp} = 49.64$	$Q_{e,cal} = 22.73$	0.76
	Second-order	Cu^{2+}	$k_1 = 0.043$	$Q_{e,exp} = 22.73$	$Q_{e,cal} = 1.65$	0.99
		Pb^{2+}	$k_2 = 0.0278$	$Q_{e,exp} = 49.64$	$Q_{e,cal} = 50.00$	1.00
Isothermal adsorption	***Langmuir***	Cu^{2+}	$K_L = 0.88$	$Q_{max} = 24.15$	---	0.99
		Pb^{2+}	$K_L = 1.31$	$Q_{max} = 90.09$	---	0.99
	Freundlich	Cu^{2+}	$K_F = 10.07$	$n = 4.68$	---	0.80
		Pb^{2+}	$K_F = 30.63$	$n = 3.02$	---	0.66

Based on the data in Table 4, it can also be predicted that the isothermal adsorption model of Cu^{2+} and Pb^{2+} ions onto BC-$KMnO_4$ fits the Langmuir model better than the Freundlich model. This is reflected in the correlation coefficient R^2 of the two corresponding mathematical equations (0,99 for both Langmuir equations of Cu^{2+} and Pb^{2+}, with the Freundlich equation only reaching 0,80 for Cu^{2+} and 0,66 for Pb^{2+}). On the other hand, from the Langmuir model equation, the maximum adsorption capacity of BC-$KMnO_4$ for Cu^{2+} ions can be extrapolated to be 24.15 $mg \cdot g^{-1}$, and for Pb^{2+} ions to be 90.09 $mg \cdot g^{-1}$, which is close to the initial concentration value for the material to reach saturation as discussed in section 3.2.3. This prediction is consistent with some previous studies (Pham et al., 2021; Song et al., 2014; Xiao et al., 2019).

In addition, the improved material adsorption capacity after modification with $KMnO_4$ solution was also observed. Specifically, in the study of the BC-MC sample in the previous research topic, the maximum adsorption capacity of the unmodified material for Cu^{2+} and Pb^{2+} ions was only 20.49 and 62.11 $mg \cdot g^{-1}$, respectively (Pham et al., 2021). This contributes to demonstrating the effectiveness of this modification method.

3.4. Comparison of the adsorption capacity of Cu^{2+} and Pb^{2+} ions on BC-$KMnO_4$

With the maximum adsorption capacity obtained from BC-$KMnO_4$ for Cu^{2+} and Pb^{2+} ions, it can be concluded that the adsorption capacity of this material for Pb^{2+} ions is better than that for Cu^{2+}. This may be related to the fact that the electronegativity of Pb is higher than that of Cu, which makes the bond between Pb^{2+} and the carbon surface stronger. Furthermore, the hydrated radius of Cu^{2+} is larger than that of Pb^{2+}, which hinders the adsorption process of Cu^{2+} ions, making the process more difficult (Ashraf et al., 2011; Inyang et al., 2012a; Pasgar et al., 2022).

This was also demonstrated through a comparative experiment of the adsorption capacity of 50 mL of a solution containing both ions simultaneously with a concentration of 100 $mg \cdot L^{-1}$. The experimental results showed that the adsorption capacity of BC-$KMnO_4$ for Cu^{2+} and Pb^{2+} was 11,9 and 33,1 $mg \cdot g^{-1}$, respectively. This value is lower than the maximum adsorption capacity value, which may be due to the competition between the metal ions with each other. A study by Y. Y. Wang et al. (2018) demonstrated that the adsorption capacity of a material for a metal ion will decrease when another metal ion is present in the adsorption solution.

4. Conclusion

Through the methods of FT-IR, EDX spectra, BET, and SEM images, the study has demonstrated that the modification process of BC-MC by $KMnO_4$ has taken place, and the initial BC-MC material has been converted to BC-$KMnO_4$. The optimal conditions for the adsorption of Cu^{2+} and Pb^{2+} ions onto BC-$KMnO_4$ are pH = 4.0, and the adsorption time is 120 minutes. The adsorption process of both metal ions onto BC-$KMnO_4$ follows the second-order kinetic model and is considered to fit the Langmuir adsorption isotherm model. The ability to adsorb Pb^{2+} ions is better than that of Cu^{2+} ions. The maximum adsorption capacity of BC-

$KMnO_4$ determined for Cu^{2+} and Pb^{2+} ions is 24.15 and 90.09 $mg \cdot g^{-1}$, respectively, higher than that of BC-MC, which is 20.45 and 62.11 $mg \cdot g^{-1}$, respectively. This shows the effectiveness of this modification method, indicating that the treatment potential of the modified material has been improved. After this study, many other research directions can be carried out: building an efficient treatment process for Cu^{2+} and Pb^{2+} ions in industrial wastewater, modifying materials with other methods to further improve the adsorption capacity of Cu^{2+} and Pb^{2+}, or expanding the study of treatment efficiency with other metal ions.

❖ ***Conflict of Interest:*** *Authors have no conflict of interest to declare.*

❖ ***Acknowledgement:*** *This research is funded by Ho Chi Minh City University of Education Foundation for Science and Technology under grant number CS.2023.19.35.*

REFERENCES

Ashraf, M. A., Wajid, A., Mahmood, K., Maah, M. J., & Yusoff, I. (2011). Low cost biosorbent banana peel (Musa sapientum) for the removal of heavy metals. *Scientific Research and Essays*, *6*(19), 4055-4064. https://doi.org/10.5897/sre11.303

Atkins, P. (2013). Physical Chemistry. In *Oxford University*. Oxford University. https://doi.org/10.1093/actrade/9780199572199.003.0002

Bakatula, E. N., Richard, D., Neculita, C. M., & Zagury, G. J. (2018). Determination of point of zero charge of natural organic materials. *Environmental Science and Pollution Research*, *25*(8), 7823-7833. https://doi.org/10.1007/s11356-017-1115-7

Barakat, M. A. (2011). New trends in removing heavy metals from industrial wastewater. *Arabian Journal of Chemistry*, *4*(4), 361-377. https://doi.org/10.1016/j.arabjc.2010.07.019

Bui. V. T., & Tran. T. X. M. (2017). Khảo sát hấp phụ As(V) trong dung dịch nước bằng vật liệu zeolite biến tính bằng Mn [Investigating the As(V) ions removal in aqueous solution using Mn-Modified zeolite material]. *Dong Thap University Journal of Science*, *24*(02-2017), 2-8.

Duwiejuah, A. B., Cobbina, S. J., & Bakobie, N. (2017). Review of eco-friendly biochar used in the removal of trace metals on aqueous phases. *International Journal of Environmental Bioremediation & Biodegradation*, *5*(2), 27–40. https://doi.org/10.12691/ijebb-5-2-1

Inyang, M., Gao, B., Yao, Y., Xue, Y., & Zimmerman, A. R. (2012a). Bioresource Technology Removal of heavy metals from aqueous solution by biochars derived from anaerobically digested biomass. *Bioresource Technology*, *110*, 50-56. https://doi.org/10.1016/j.biortech.2012.01.072

Inyang, M., Gao, B., Yao, Y., Xue, Y., Zimmerman, A. R., Pullammanappallil, P., & Cao, X. (2012b). Removal of heavy metals from aqueous solution by biochars derived from anaerobically digested biomass. *Bioresource Technology*, *110*, 50–56. https://doi.org/10.1016/j.biortech.2012.01.072

Keiluweit, M., Nico, P. S., Johnson, M. G., & Kleber, M. (2010). Dynamic Molecular Structure of Plant Biomass-derived Black Carbon(Biochar)- Supporting Information -. *Environ. Sci. Technol.*, *44*(4), 1247–1253. 10.1021/es9031419

Kumar, R., Rani, M., Gupta, H., & Gupta, B. (2014). Trace metal fractionation in water and sediments of an urban river stretch. *Chemical Speciation and Bioavailability*, *26*(4), 200-209. https://doi.org/10.3184/095422914X14142369069568

Li, B., Yang, L., Wang, C.-Q., Zhang, Q.-P., Liu, Q.-C., Li, Y.-D., & Xiao, R. (2017). Adsorption of Cd(II) from aqueous solutions by rape straw biochar derived from different modification processes. *Chemosphere*, *175*, 332–340. https://doi.org/10.1016/j.chemosphere.2017.02.061

Li, H., Dong, X., da Silva, E. B., de Oliveira, L. M., Chen, Y., & Ma, L. Q. (2017). Mechanisms of metal sorption by biochars: Biochar characteristics and modifications. *Chemosphere*, *178*, 466–478. https://doi.org/10.1016/j.chemosphere.2017.03.072

Ma, J., Huang, W., Zhang, X., Li, Y., & Wang, N. (2021). The utilization of lobster shell to prepare low-cost biochar for high-efficient removal of copper and cadmium from aqueous: Sorption properties and mechanisms. *Journal of Environmental Chemical Engineering*, *9*(1), 104703. https://doi.org/10.1016/j.jece.2020.104703

Merck. (2022). *IR Spectrum Table & Chart*. https://www.sigmaaldrich.com/VN/en/technical-documents/technical-article/analytical-chemistry/photometry-and-reflectometry/ir-spectrum-table

Ni, B., Huang, Q., Wang, C., Ni, T., Sun, J., & Wei, W. (2019). Chemosphere Competitive adsorption of heavy metals in aqueous solution onto biochar derived from anaerobically digested sludge. *Chemosphere*, *219*, 351-357. https://doi.org/10.1016/j.chemosphere.2018.12.053

Pasgar, A., Nasiri, A., & Javid, N. (2022). Single and competitive adsorption of Cu^{2+} and Pb^{2+} by tea pulp from aqueous solutions. *Environmental Health Engineering and Management*, *9*(1), 65–74. https://doi.org/10.34172/EHEM.2022.08

Pham, T. C. L., Luu, G. H., Nguyen, K. D. M., & Truong, C. H. (2021). Nghiên cứu khả năng xử lí ion Pb(II) và Cu(II) trong dung dịch bằng than sinh học điều chế từ mùn cưa [A study on the removal of ions Pb(II) and Cu(II) from solution by using biochar derived from sawdust]. *Ho Chi Minh City University of Education Journal of Science*, *12*, 2162-2177.

Song, Z., Lian, F., Yu, Z., Zhu, L., Xing, B., & Qiu, W. (2014). Synthesis and characterization of a novel MnOx-loaded biochar and its adsorption properties for Cu^{2+} in aqueous solution. *Chemical Engineering Journal*, *242*, 36-42. https://doi.org/10.1016/j.cej.2013.12.061

Sun, C., Chen, T., Huang, Q., Wang, J., Lu, S., & Yan, J. (2019). Enhanced adsorption for Pb(II) and Cd(II) of magnetic rice husk biochar by KMnO4 modification. *Environmental Science and Pollution Research*, *26*(9), 8902-8913. https://doi.org/10.1007/s11356-019-04321-z

Tan, X.-F., Liu, Y.-G., Gu, Y.-L., Xu, Y., Zeng, G.-M., Hu, X.-J., Liu, S.-B., Wang, X., Liu, S.-M., & Li, J. (2016). Biochar-based nano-composites for the decontamination of wastewater: A review. *Bioresource Technology*, *212*, 318–333. https://doi.org/10.1016/j.biortech.2016.04.093

Wang, S., Gao, B., Li, Y., Mosa, A., Zimmerman, A. R., Ma, L. Q., Harris, W. G., & Migliaccio, K. W. (2015). Manganese oxide-modified biochars: Preparation, characterization, and sorption of arsenate and lead. *Bioresource Technology*, *181*, 13-17. https://doi.org/10.1016/j.biortech.2015.01.044

Wang, Y., Liu, Y., Lu, H., Yang, R., & Yang, S. (2018). Competitive adsorption of Pb (II), Cu (II, and Zn (II) ions onto hydroxyapatite-biochar nanocomposite in aqueous solutions. *Journal of Solid State Chemistry*, *261*(February), 53-61. https://doi.org/10.1016/j.jssc.2018.02.010

Wang, Y.-Y., Liu, Y.-X., Lu, H.-H., Yang, R.-Q., & Yang, S.-M. (2018). Competitive adsorption of Pb(II), Cu(II), and Zn(II) ions onto hydroxyapatite-biochar nanocomposite in aqueous solutions. *Journal of Solid State Chemistry*, *261*, 53–61. https://doi.org/10.1016/j.jssc.2018.02.010

Xiao, Z., Zhang, L., Wu, L., & Chen, D. (2019). Adsorptive removal of Cu(II) from aqueous solutions using a novel macroporous bead adsorbent based on poly(vinyl alcohol)/sodium alginate/KMnO4 modified biochar. *Journal of the Taiwan Institute of Chemical Engineers*, *102*, 110-117. https://doi.org/10.1016/j.jtice.2019.05.010

NGHIÊN CỨU CẢI TIẾN KHẢ NĂNG XỬ LÍ ION Pb^{2+} VÀ Cu^{2+} TRONG DUNG DỊCH CỦA THAN SINH HỌC CÓ NGUỒN GỐC TỪ MÙN CƯA BẰNG PHƯƠNG PHÁP BIẾN TÍNH VỚI $KMnO_4$

Lưu Gia Hy[1], Phạm Tăng Cát Lượng[2], Trương Chí Hiền[1], Nguyễn Thị Bạch Mai[3] Nguyễn Kim Diễm Mai[1*]

[1]Trường Đại học Sư phạm Thành phố Hồ Chí Minh, Việt Nam

[2]Trường Đại học Bách khoa, Đại học Quốc gia Thành phố Hồ Chí Minh, Việt Nam

[3] Trường Đại học Nông Lâm Thành phố Hồ Chí Minh, Việt Nam

[*]Tác giả liên hệ: Nguyễn Kim Diễm Mai – Email: mainkd@hcmue.edu.vn

Ngày nhận bài: 09-7-2024; Ngày nhận bài sửa: 08-9-2024; Ngày duyệt đăng: 01-10-2024

TÓM TẮT

Nghiên cứu này cải tiến than sinh học có nguồn gốc từ mùn cưa BC-MC bằng cách biến tính với $KMnO_4$ để tạo thành BC-$KMnO_4$. Sau đó khảo sát các yếu tố tác động đến quá trình hấp phụ ion Cu^{2+} và Pb^{2+} trên vật liệu than được cải tiến. Các yếu tố khảo sát bao gồm: giá trị pH (2,0 – 6,0), nồng độ đầu ion kim loại (25 – 200 $mg{\cdot}L^{-1}$), thời gian hấp phụ (5 – 1440 phút) và khối lượng than sinh học (0,05 – 0,10 g). Nghiên cứu chỉ ra quá trình hấp phụ ion Cu^{2+}và Pb^{2+} của BC-$KMnO_4$ tuân theo quy luật động học bậc hai và mô hình đẳng nhiệt hấp phụ Langmuir. Kết quả cho thấy dung lượng hấp phụ cực đại của BC-$KMnO_4$ đạt 24,15 $mg{\cdot}g^{-1}$ đối với Cu^{2+} và 90,09 $mg{\cdot}g^{-1}$ đối với Pb^{2+}. Giá trị dung lượng hấp phụ cực đại này đã có sự cải thiện so với của BC-MC. Nghiên cứu này cũng so sánh khả năng hấp phụ của vật liệu đối với ion Cu^{2+}và Pb^{2+}.

Từ khoá: Hấp phụ; than sinh học; ion Cu^{2+}; ion Pb^{2+}; biến tính với $KMnO_4$.